Supplemental Figure 1. Surface expression of AE2 RL1 mutants does not differ from that of wild-type AE2. **A**. Upper panel: normalized, water-subtracted GFP fluorescence intensity (AFU; arbitrary fluorescence units) at periphery of oocytes expressing AE2-^{1075}AAAQN^{1079}-GFP compared to that of oocytes expressing wildtype AE2-GFP ($p > 0.05$, unpaired Student's t-test). Lower panels: Confocal images of representative oocytes expressing C-terminal GFP fusion proteins of wildtype AE2 and of AE2 mutant ^{1075}AAAQN^{1079}. Bar, 100 μm. **B**. Upper panel: normalized, water-subtracted fluorescence intensity of immunostained oocytes expressing ecto-loop-HA-tagged wildtype or mutant AE2 constructs previously injected with the indicated amounts of cRNA ($p > 0.05$, Dunnett`s t-test). Lower panels: confocal images of representative immunostained oocytes expressing HA-tagged wildtype AE2 or AE2-RL1 mutants. Bar, 100 μm.

Supplemental Figure 2. RL1 residues of AE3 are also important for acute regulation by pH. *A,* Time course of $^{36}Cl^-$ efflux from representative individual oocytes expressing wildtype cAE3 (circles) or cAE3 RL1 mutant ^{869}AAAQN^{873} (squares) during elevation of pH_i by removal of 40 mM butyrate, with subsequent exposure to DIDS (200 μM). *B*, Normalized $^{36}Cl^-$ efflux rate constants (± S.E.) in the presence of 40 mM butyrate for (n) oocytes expressing wildtype AE2, wildtype AE3, or the indicated RL1 mutant polypeptides. Gray bars indicate $p<0.05$ compared to the corresponding wildtype AE. The data for wildtype AE2 and AE2-AAAQN are reproduced from Figure 3C for comparison.

Supplemental Figure 3. Rate constants for $^{36}Cl^-$ efflux at pH_o 7.4 from oocytes encoding wildtype AE2 or the indicated AE2 substitution mutants. Oocytes were injected with the cRNA quantities noted inside the bars, chosen to approximate the $^{36}Cl^-$ efflux rate constant at pH_o 7.4 of oocytes injected with 10 ng cRNA encoding wildtype AE2. This allowed comparison of regulation by pH of wildtype and mutant AE polypeptides measured at equivalent levels of activity. With the exception of AE2 mutant K1078Q, which showed a moderate reduction in activity, efflux rate constants for these AE2 missense mutants did not differ from that of wildtype AE2 ($p > 0.05$, Dunnett's t-test). B. Resting pH_i, as measured with pH_i microelectrodes (10) did not differ between oocytes expressing wildtype AE2 or the indicated AE2 RL1 mutants. "*AE2 wt" indicates data taken from (10) and does not differ from the present measurements (Dunnetts t-test, $p > 0.05$). C. Magnitude (ΔpH_i) of butyrate-induced intracellular acidification did not differ significantly in oocytes previously injected with H_20 or with cRNA encoding wildtype AE2 or AE2 RL1 mutants (Dunnetts t-test, $p > 0.05$).

Supplemental Figure 4. Correlation of $pH_{o(50)}$ values of AE2 I1079 substitution mutants with side chain solvation free energies. A. $pH_{o(50)}$ correlation with normalized water-to-phosphatidylcholine interfacial free energy of model pentapeptide AcWL-X-LL, in which X is the substituent aa at AE2 position 1079.

B. $pH_{o(50)}$ correlation with normalized water-to-octanol interfacial free energy of peptide AcWL-X-LL, in which X is the substituent aa at AE2 position 1079. These experimentally derived transfer free energy values are from Figure 8 of (26), and may assess an index of I1079 accessibility to extracellular solution.

Supplemental Figure 1

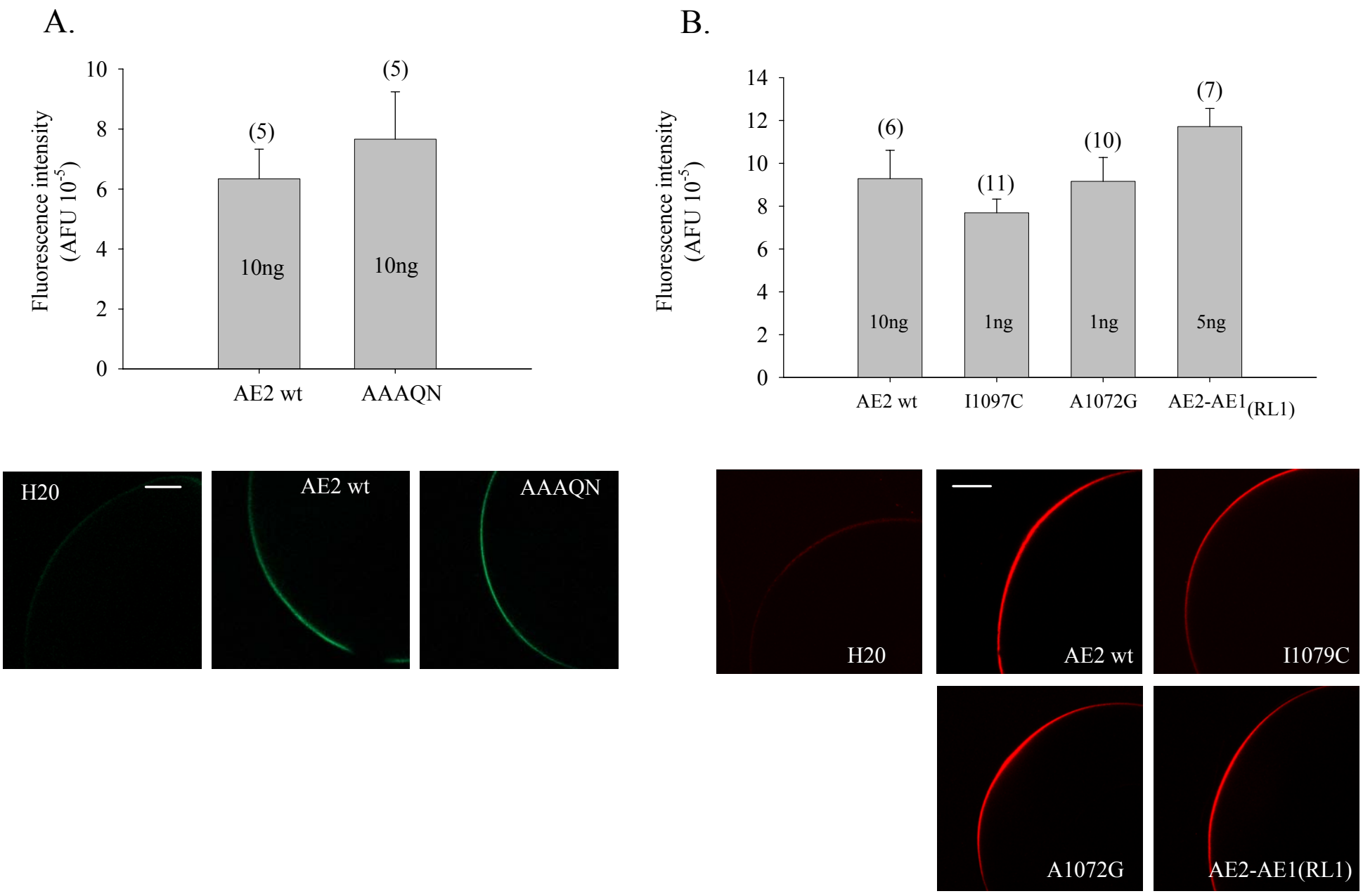

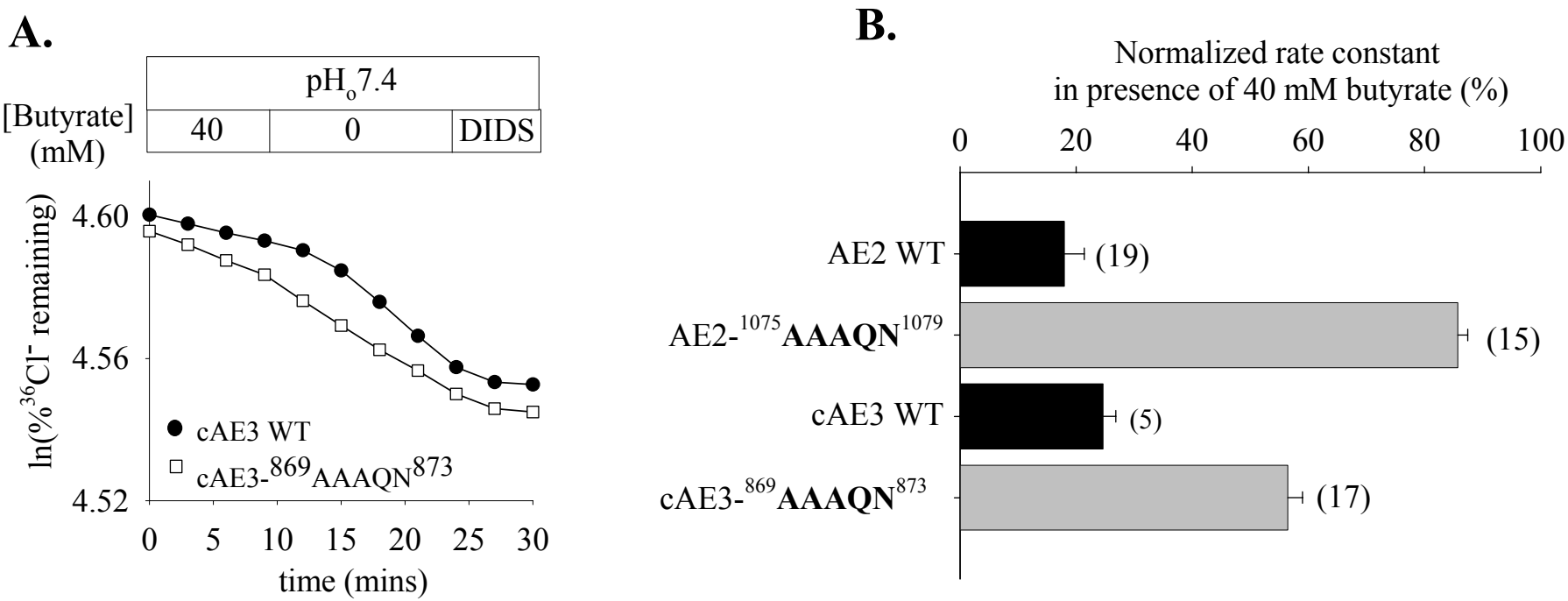
A.
pHo7.4
[Butyrate] (mM)
40
0
DIDS
ln(%36Cl- remaining)
4.60
4.56
4.52
cAE3 WT
cAE3-869AAAQN873
0
5
10
15
20
25
30
time (mins)
B.
Normalized rate constant
in presence of 40 mM butyrate (%)
0
20
40
60
80
100
AE2 WT
(19)
AE2-1075AAAQN1079
(15)
cAE3 WT
(5)
cAE3-869AAAQN873
(17)

Supplemental Figure 3

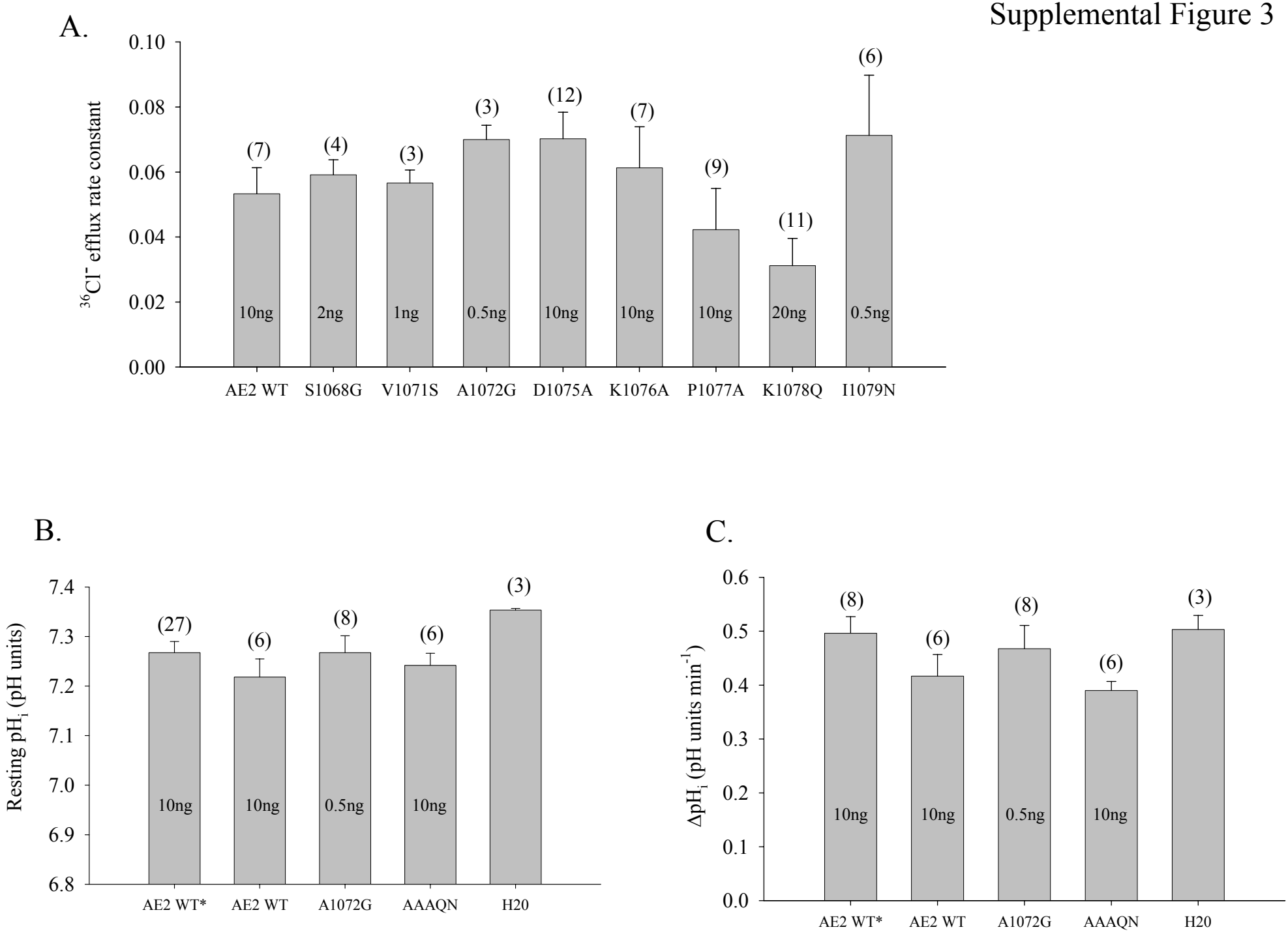

Supplemental Figure 4

A.

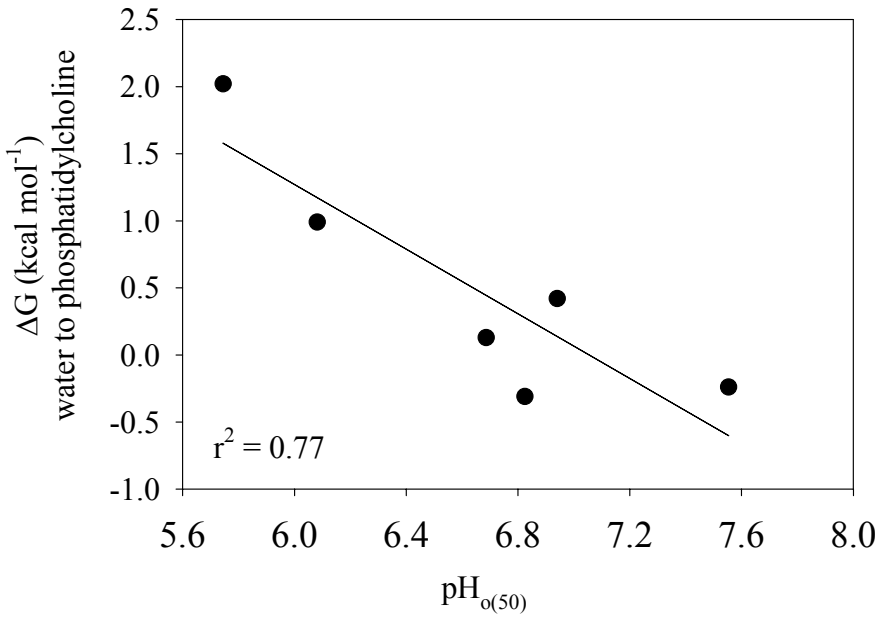

B.